Supplementary Information

for

Reversible interconversion of pharmaceutical salt polymorphs facilitated by mechanical methods

Liulei Ma, Qixuan Zheng, Daniel K. Unruh, and Kristin M. Hutchins*

Department of Chemistry and Biochemistry, Texas Tech University, 1204 Boston Avenue, Lubbock, TX 79409, United States.

*Email: kristin.hutchins@ttu.edu

1. Experimental details Page S1-S3

2. X-ray diffraction information and data tables Page S4-S5

3. Single-crystal X-ray structures Page S6-S7

4. NMR data for salts Page S8-S9

5. Single-crystal X-ray structures of layered assemblies Page S10

6. TGA data Page S11-S13

7. DTA data Page S14-S16

8. FTIR spectra of components and salts Page S17

9. Solubility studies Page S18

10. PXRD patterns Page S19-S25

11. Crystal imaging experiments Page S26

12. References Page S27

1. Experimental details

Materials

Trimethoprim (**TMP**), D-(-)-Lactic acid (**DLA**, 90%), L-(+)-Lactic acid (**LLA**, 95%) were purchased from AA Blocks Chemical (San Diego, CA, USA). Acetonitrile, 2-propanol, dichloromethane, acetone, ethyl acetate, methanol and ethanol were purchased from Fisher Scientific (Fair Lawn, NJ, USA). Nitromethane was purchased from Oakwood Chemical (Columbia, SC, USA).

Neat milling experiments

A FlackTek SpeedMixer 330-100 SE purchased from FlackTek manufacturing was used. Experiments were conducted in 15 mL stainless steel jars with two 7 mm stainless steel grinding balls using a custom holder acquired from FlackTek. In 1:1 molar ratio, **TMP** (95.8 mg, 0.33 mmol), **DLA** (33.0 mg, 0.33 mmol) or **LLA** (31.3 mg, 0.33 mmol) were placed in a stainless-steel jar. The mixture was milled at 1500 rpm for a period of 15 min. PXRD performed immediately after milling or after leaving on the bench for several hours gave identical patterns.

Liquid-assisted grinding (LAG) experiments

Experiments were conducted in 15 mL stainless steel jars with two 7 mm stainless steel grinding balls using a custom holder acquired from FlackTek. In 1:1 molar ratio, **TMP** (95.8 mg, 0.33 mmol), **DLA** (33.0 mg, 0.33 mmol) or **LLA** (31.3 mg, 0.33 mmol), and 50 µL of acetonitrile or ethanol were placed in a stainless-steel jar. The mixture was milled at 1500 rpm for a period of 15 min. The solid obtained from milling has a waxy appearance. PXRD performed immediately after milling or after leaving on the bench for several hours gave identical patterns. Alpha forms of the salts were obtained from LAG using ethanol, while the beta forms of the salts were obtained from LAG using acetonitrile.

Slurry experimental method

Slurry experiments were performed by combining **TMP** (95.8 mg, 0.33 mmol) with **DLA** (40.0 mg, 0.40 mmol) or **LLA** (37.9 mg, 0.40 mmol) in a 1:1.2 molar ratio in a 20 mL glass scintillation vial with a stir bar. For each slurry, a volume of 2-4 mL of ethanol or acetonitrile was added to the vial, and the slurry was stirred for 24 h. The slurry was then filtered, washed with the solvent used for that slurry, and air dried before being analyzed by PXRD. Alpha forms of the salts were obtained by performing slurry experiments in ethanol, while beta forms of the salts were obtained by performing slurry experiments in acetonitrile.

Mechanochemical polymorph interconversion

Experiments were conducted in 15 mL stainless steel jars with two 7 mm stainless steel grinding balls using a custom holder acquired from FlackTek. 100-120 mg crystalline powder of **TMP·DLA** or **TMP·LLA**, and 100 µL of acetonitrile/H_2O (v/v, 5:1) or methanol were placed in a stainless-steel jar. The mixture was milled at 1500 rpm for a period of 15 min. The steel jars are left open on the bench for several hours, and air dried before being analyzed by PXRD.

α forms of salts to **β** forms of salts: acetonitrile/H_2O (v/v, 5:1)

β forms of salts to **α** forms of salts: methanol

Slurry polymorph interconversion

Experiments were performed by adding 60-120 mg crystalline powder of **TMP·DLA** or **TMP·LLA** in a 20 mL glass scintillation vial with a stir bar. For each slurry, a volume of 1-4 mL of acetonitrile/H_2O (v/v, 20:1) or ethanol was added to the vial, and the slurry was stirred for 24 h. The slurry was then filtered, washed with the solvent used for that slurry, and air dried before being analyzed by PXRD.

α forms of salts to **β** forms of salts: acetonitrile/H_2O (v/v, 20:1)

β forms of salts to **α** forms of salts: ethanol

Salification

All crystallization experiments were conducted at ambient humidity unless specifically mentioned.

Slow evaporation: **TMP·DLA** and **TMP·LLA** were grown by dissolving **TMP** (15 mg, 0.05 mmol), and **DLA** (5 mg, 0.05 mmol) or **LLA** (5 mg, 0.05 mmol) in ~10 mL methanol or ethanol. Slow evaporation of the solution was allowed for a period of 4-7 days until single crystals were formed that were suitable for X-ray diffraction. These two solvents afforded one polymorph at times, and at other times a mixture of polymorphs formed.

Salts of **TMP·DLA(α)** or **TMP·LLA(α)** were grown by dissolving ~10 mg of dried alpha crystalline powder (obtained from slurry or liquid-assisted grinding) in 5-10 mL ethanol. Slow evaporation of the solution was allowed at room temperature for a period of 4-7 days until single crystals were formed that were suitable for X-ray diffraction.

Salts of **TMP·DLA(β)** or **TMP·LLA(β)** were obtained by dissolving ~5 mg of dried beta crystalline powder (obtained from slurry or liquid-assisted grinding) in the mixture of 0.5 mL 2-propanol and H_2O (v/v, 20:1). The solution was placed on a hotplate at ~50-60 °C and subjected to fast evaporation (no cap on the vial) for a period of 8-12 h until single crystals were formed that were suitable for X-ray diffraction. However, alpha forms of the salts can occasionally be obtained by this method.

Table S1. Results from liquid-assisted grinding (LAG) and slurry experiments using **TMP** and **DLA** or **LLA** in different solvents.

Solvent	**Product (LAG)**	**Product (slurry)**
ethanol	alpha	alpha
acetonitrile	beta	beta
acetone	alpha	alpha
dichloromethane	alpha	beta
ethyl acetate	alpha	beta
2-propanol	alpha	beta
nitromethane	beta	beta

2. X-ray diffraction information and data tables

Data were collected on a Rigaku XtaLAB Synergy-*i* Kappa diffractometer equipped with a PhotonJet-*i* X-ray source operated at 50 W (50 kV, 1 mA) to generate Cu Kα radiation (λ = 1.54178 Å) and a HyPix-6000HE HPC detector. Crystals were transferred from the vial and placed on a glass slide in type NVH immersion oil by Cargille. A Zeiss Stemi 305 microscope was used to identify a suitable specimen for X-ray diffraction from a representative sample of the material. The crystal and a small amount of the oil were collected on a Hampton Research 20 micron nylon CryoLoop and transferred to the instrument where it was placed under a cold nitrogen stream (Oxford 700 series) maintained at 100 K throughout the duration of the experiment. The sample was optically centered with the aid of a video camera to insure that no translations were observed as the crystal was rotated through all positions. A unit cell collection was then carried out. After it was determined that the unit cell was not present in the CCDC database a data collection strategy was calculated by *CrysAlis*^{Pro}.[1] The crystal was measured for size, morphology, and color.

Refinement Details

After data collection, the unit cell was re-determined using a subset of the full data collection. Intensity data were corrected for Lorentz, polarization, and background effects using *CrysAlis*^{Pro}.[1] A numerical absorption correction was applied based on a Gaussian integration over a multifaceted crystal and followed by a semi-empirical correction for adsorption applied using the program *SCALE3 ABSPACK*.[2] The program *SHELXT*[3] was used for the initial structure solution and *SHELXL*[4] was used for refinement of the structure. Both of these programs were utilized within the OLEX2[5] software. Hydrogen atoms bound to carbon, nitrogen, and oxygen atoms were located in the difference Fourier map and were geometrically constrained using the appropriate AFIX commands.

In each salt, one of the two crystallographically unique lactic acid molecules is disordered, and the molecule is disordered over two positions. The same restraints were applied to each polymorph for consistency. The intermolecular hydrogen bonds to neighboring trimethoprim and lactic acid molecules is retained.

For **TMP·DLA(α)**, the **DLA** molecule (O10 < O12 and C32 < C34) was positionally disordered over two sites (A and B). The site occupancies for these sites were constrained to 0.5, and the rigid bond restraint RIGU was also applied to the disordered sites.

For **TMP·DLA(β)**, the **DLA** molecule (O10 < O12 and C32 < C34) was positionally disordered over two sites (A and B). The site occupancies for the A and B sites refined to 0.71 and 0.29, respectively. To help maintain reasonable ADP values, the rigid bond restraint RIGU was applied to the disordered sites.

For **TMP·LLA(α)**, the **LLA** molecule (O10 < O12 and C32 < C34) was positionally disordered over two sites (A and B). The site occupancies for the A and B sites refined to 0.63 and 0.37, respectively. The rigid bond restraint RIGU was also applied to the disordered sites.

For **TMP·LLA(β)**, the **LLA** molecule (O10 < O12 and C32 < C34) was positionally disordered over two sites (A and B). The site occupancies for the A and B sites refined to 0.72 and 0.28, respectively. The rigid bond restraint RIGU was also applied to the disordered sites.

Table S2. X-ray data for **TMP·DLA(α)**, **TMP·DLA(β)**, **TMP·LLA(α)**, and **TMP·LLA(β)**.

compound name	**TMP·DLA(α)**	**TMP·DLA(β)**	**TMP·LLA(α)**	**TMP·LLA(β)**
chemical formula	$C_{17}H_{24}N_4O_6$	$C_{17}H_{24}N_4O_6$	$C_{17}H_{24}N_4O_6$	$C_{17}H_{24}N_4O_6$
formula weight	380.40	380.40	380.40	380.40
crystal system	Monoclinic	Triclinic	Monoclinic	Triclinic
space group	*P2₁*	*P1*	*P2₁*	*P1*
a/Å	5.0975	5.0684	5.0732	5.0665
b/Å	36.4142	9.7499	36.4013	9.7541
c/Å	10.0043	19.4419	10.0547	19.4423
α/°	90.000	85.504	90.000	85.388
β/°	95.264	88.829	95.365	88.841
γ/°	90.000	77.838	90.000	77.804
V/Å^3	1849.18	936.29	1848.68	936.09
P_{calc}/g cm^{-3}	1.366	1.349	1.367	1.350
T/K	100.00	100.00	100.01	99.96
Z	4	2	1	2
radiation type	Cu Kα	Cu Kα	Cu Kα	Cu Kα
absorption coefficient, μ/mm^{-1}	0.878	0.867	0.878	0.867
no. of reflections measured	18312	30525	46670	54448
no. of independent reflections	6107	6256	7459	6761
no. of reflection (I>2σ(I))	5538	5733	6982	6060
R_{int}	0.0321	0.0480	0.0389	0.0681
R_1 ((I>=2σ(I))	0.0344	0.0369	0.0338	0.0439
wR(F^2) (I>=2σ(I))	0.0919	0.0958	0.0868	0.1157
R_1 (all data)	0.0396	0.0425	0.0371	0.0503
wR(F^2) (all data)	0.0945	0.1024	0.0886	0.1223
Goodness-of-fit	1.058	1.051	1.055	1.036
CCDC deposition number	2241034	2241035	2241036	2241037

3. Single-crystal X-ray structures

For the thermal ellipsoid images below, carbon, hydrogen, oxygen, and nitrogen atoms are represented by gray, white, red, and light blue ellipsoids, respectively.

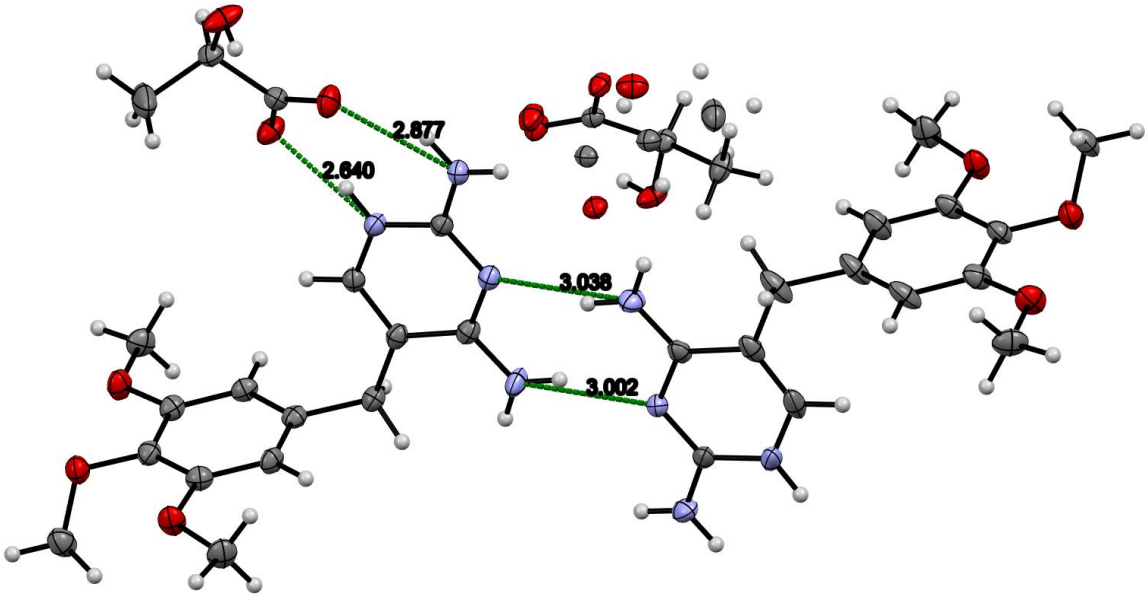

Fig. S1 Asymmetric unit of **TMP·DLA(α)** at 100 K with thermal ellipsoids plotted at 50% probability.

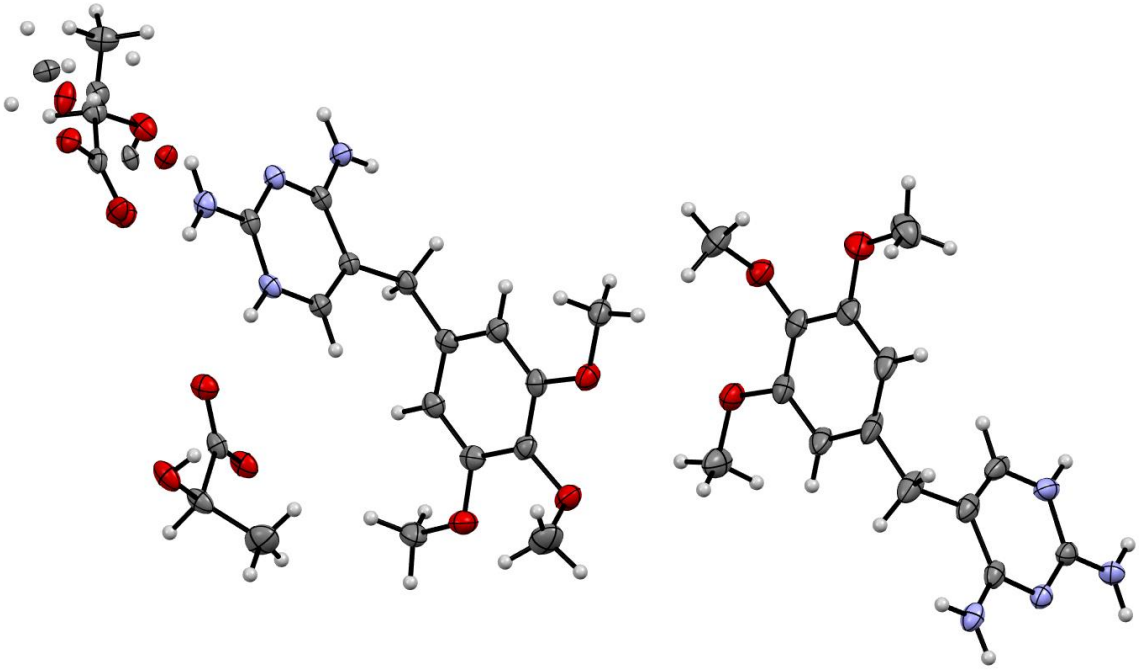

Fig. S2 Asymmetric unit of **TMP·DLA(β)** at 100 K with thermal ellipsoids plotted at 50% probability.

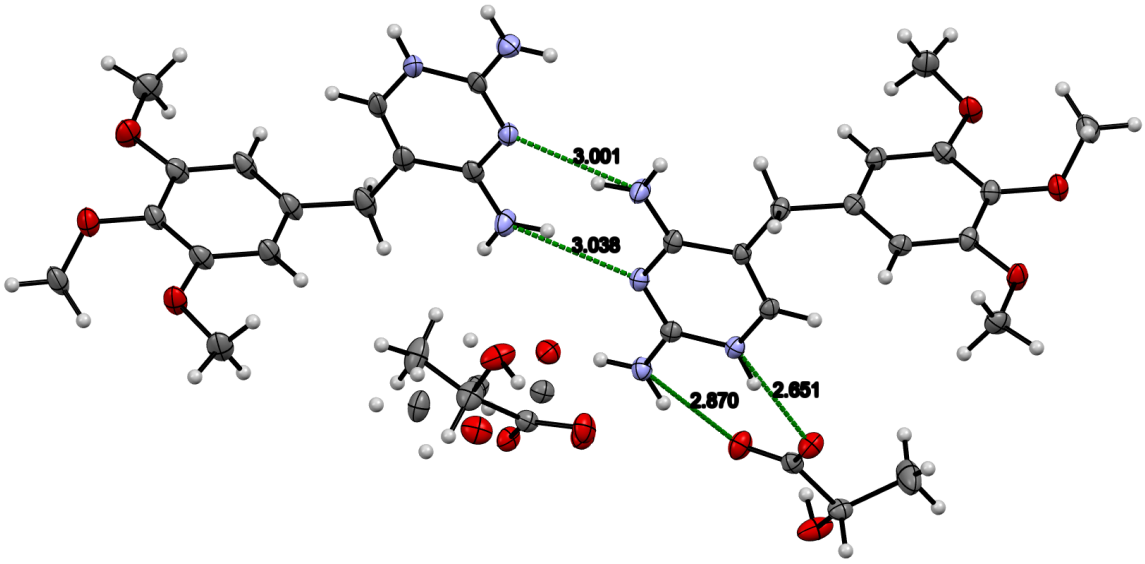

Fig. S3 Asymmetric unit of **TMP·LLA(α)** at 100 K with thermal ellipsoids plotted at 50% probability.

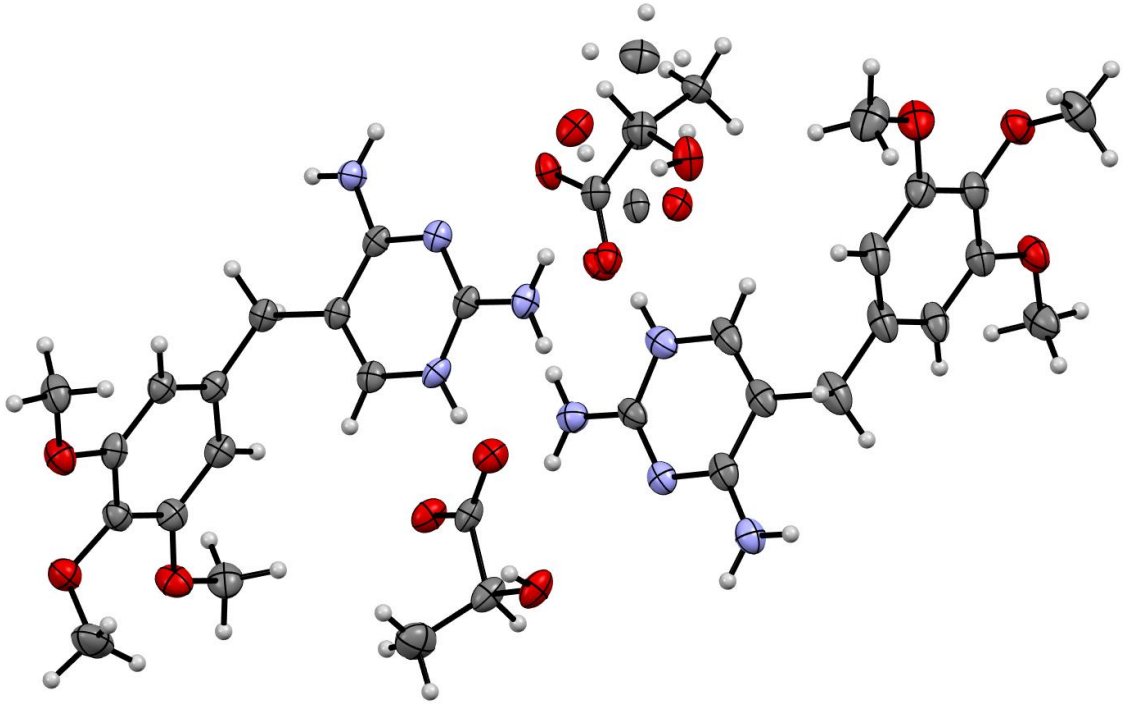

Fig. S4 Asymmetric unit of **TMP·LLA(β)** at 100 K with thermal ellipsoids plotted at 50% probability.

4. NMR data for salts

Single crystals from the salification experiments were removed from the vials and dissolved in DMSO-d_6 for ^{1}H NMR experiments. NMR data was collected using a JOEL ECS 400 MHz Spectrometer.

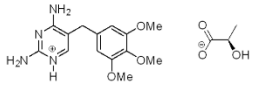

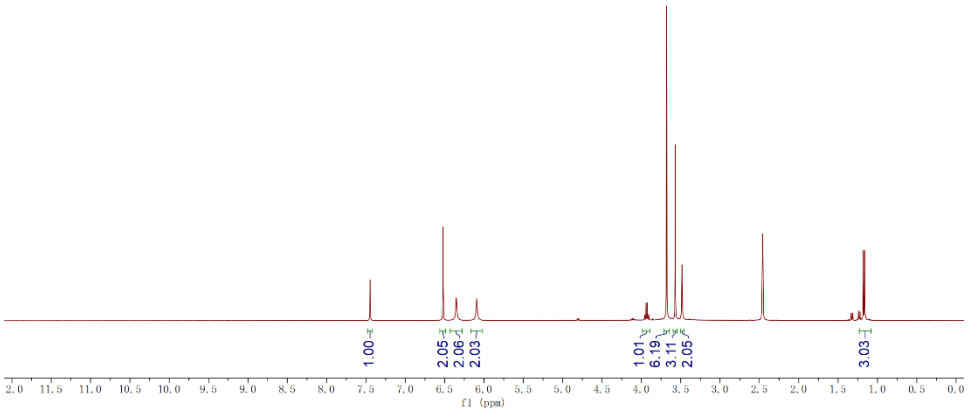

Fig. S5 ^{1}H NMR spectrum of **TMP·DLA(α)**.

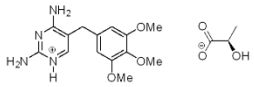

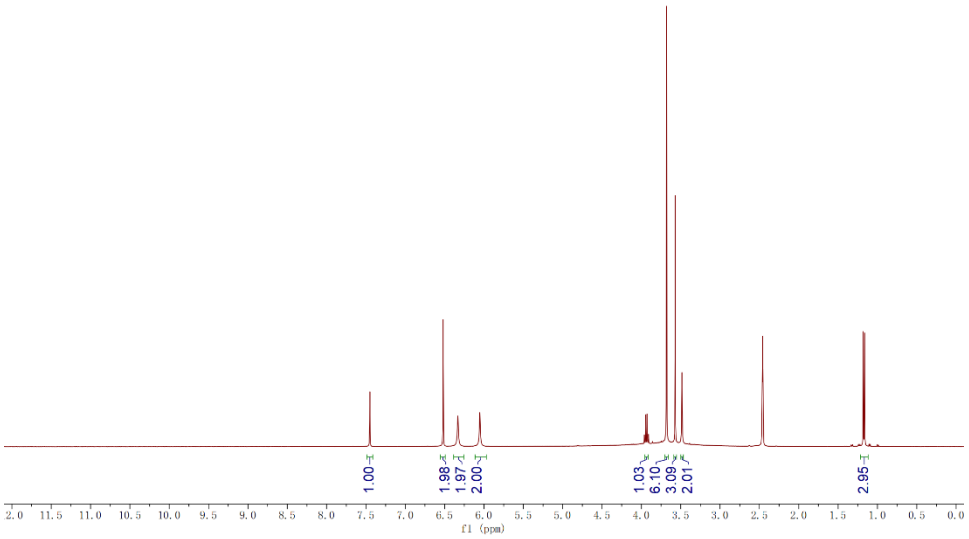

Fig. S6 ^{1}H NMR spectrum of **TMP·DLA(β)**.

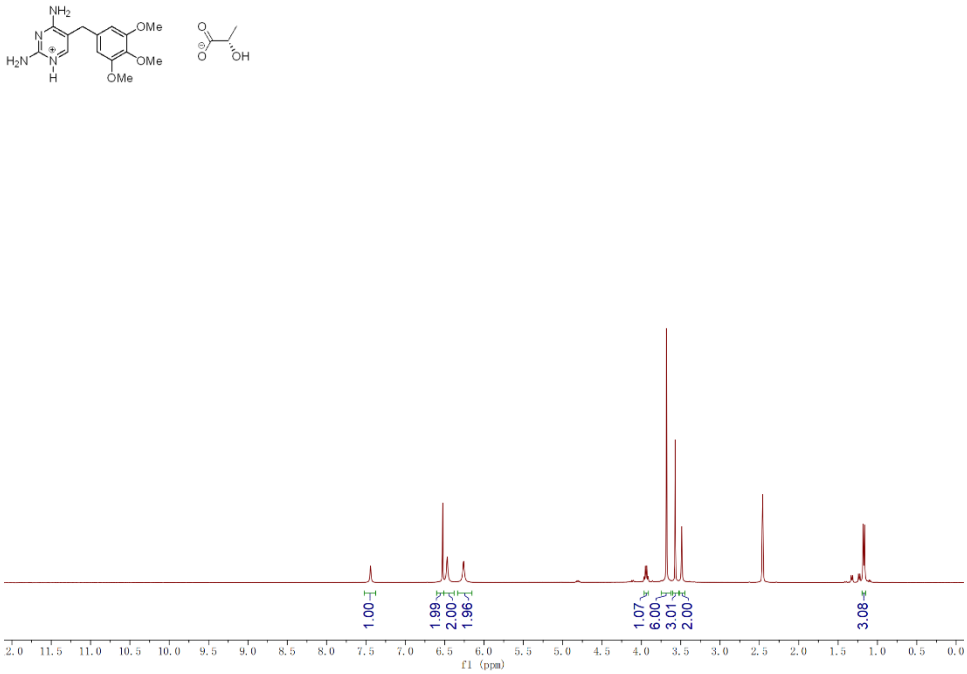

Fig. S7 ^{1}H NMR spectrum of **TMP·LLA(α)**.

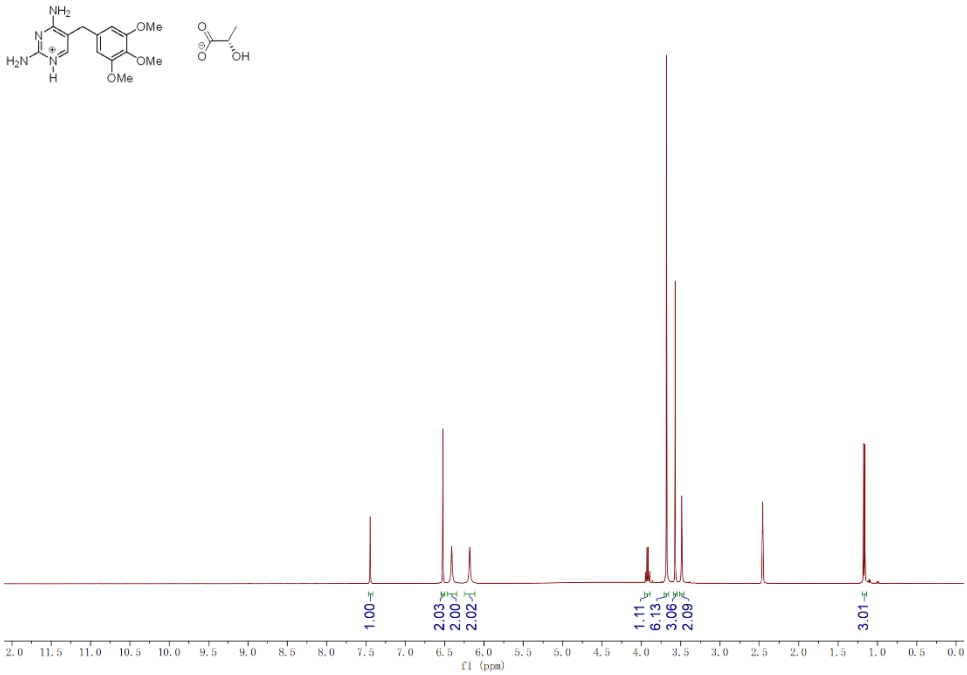

Fig. S8 ^{1}H NMR spectrum of **TMP·LLA(β)**.

5. Single-crystal X-ray structures of layered assemblies

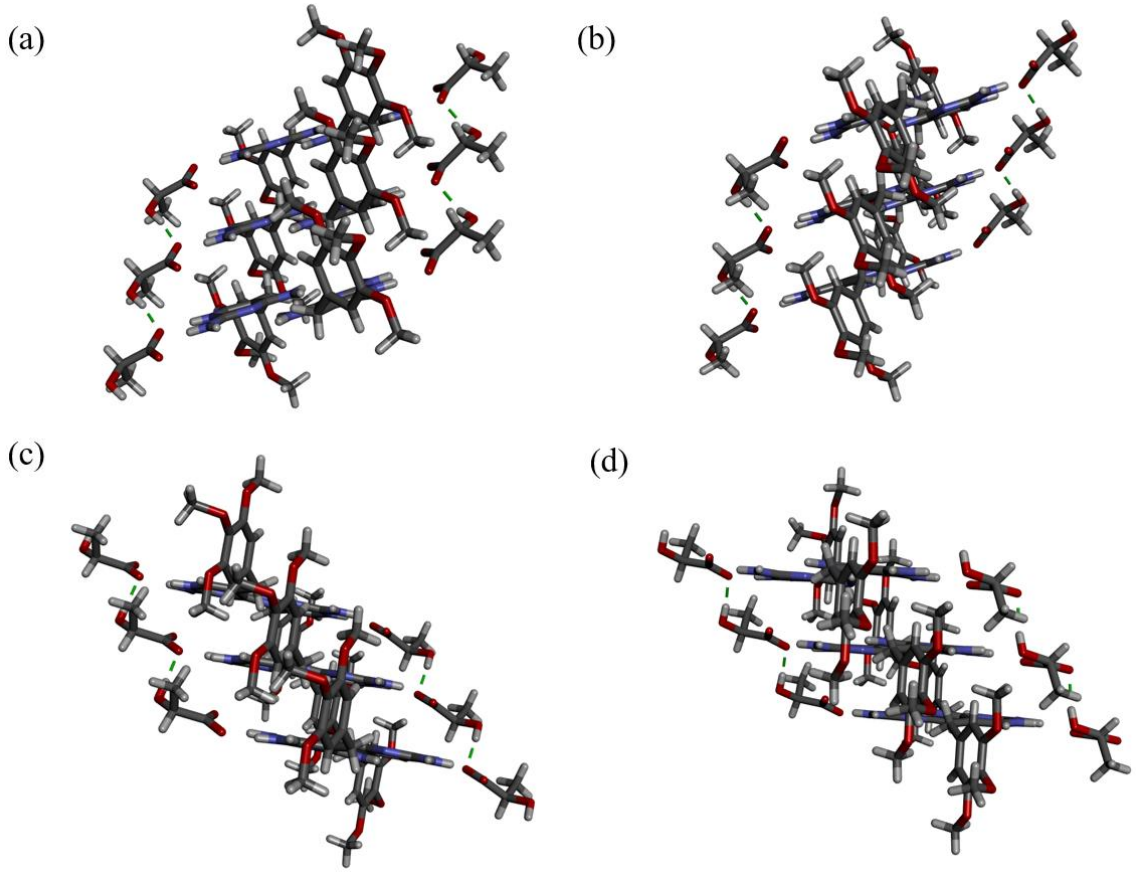

Fig. S9 X-ray crystal structures showing layers of: (a) **TMP·DLA(α)**, (b) **TMP·LLA(α)**, (c) **TMP·DLA(β)** and (d) **TMP·LLA(β)**. Hydrogen bonds shown with green dashed lines. Disorder in the four salts is omitted for clarity.

6. TGA thermograms

TGA data was collected on a SHIMADZU DTG_60H instrument. An alumina cell and a nitrogen atmosphere were used. The flow rate was 100 mL/min, and the heating rate was 10 °C/min. The onset temperature is listed for each sample under the thermogram.

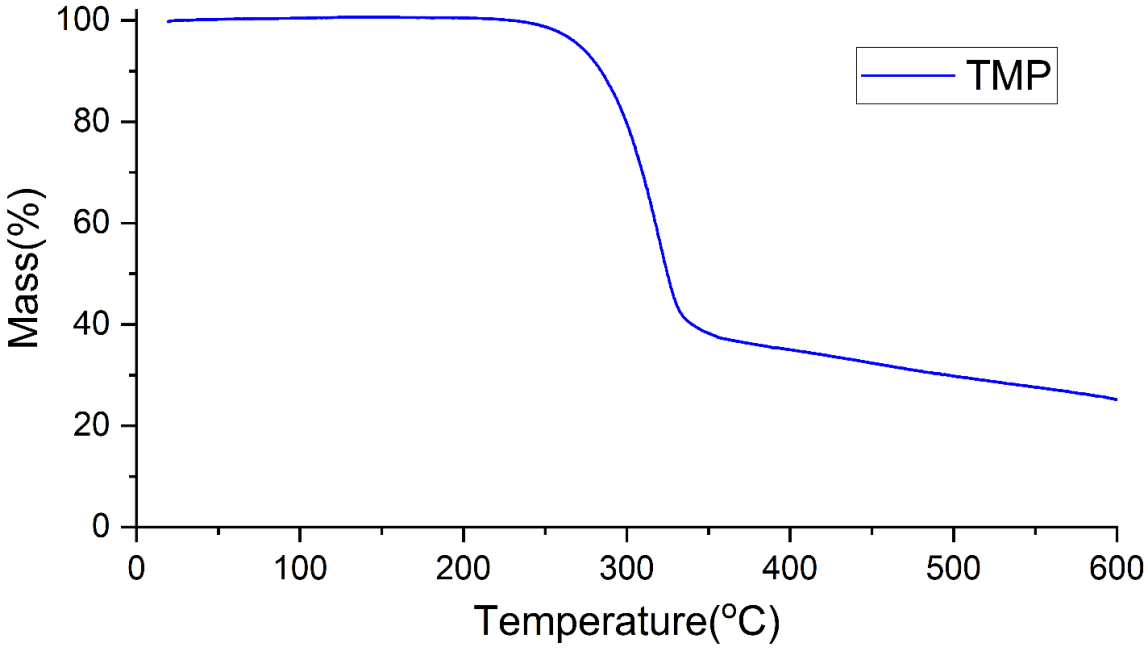

Fig. S10 TGA thermogram for **TMP**. Decomposition began at ca. 278°C.

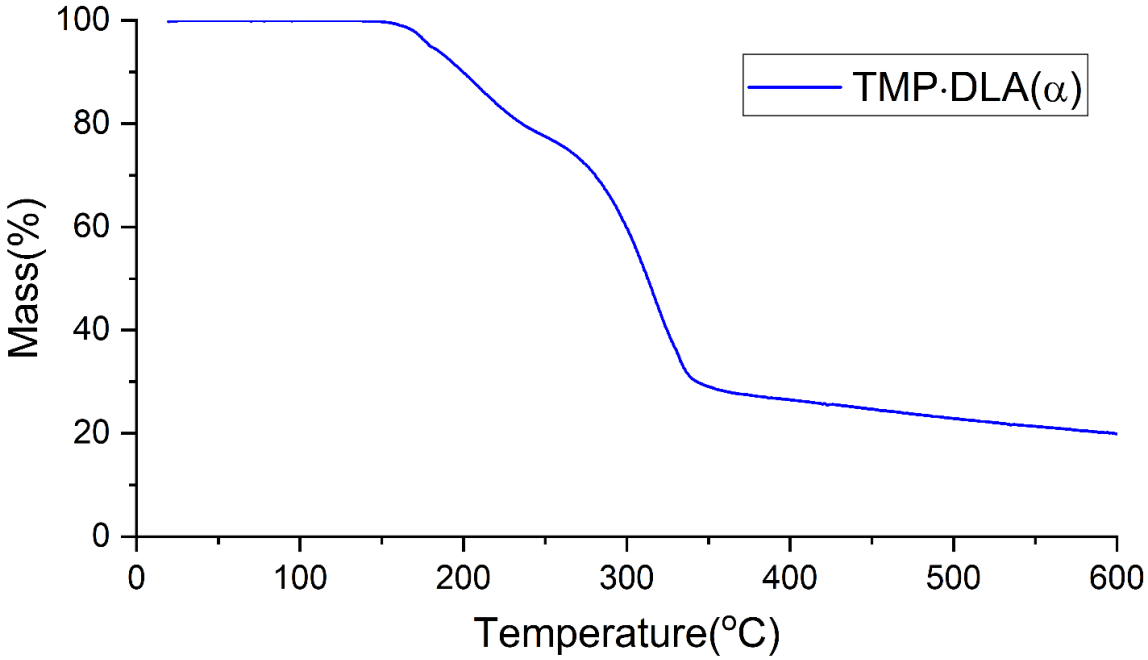

Fig. S11 TGA thermogram for **TMP·DLA(α)**. Crystal decomposition began at ca. 169 °C.

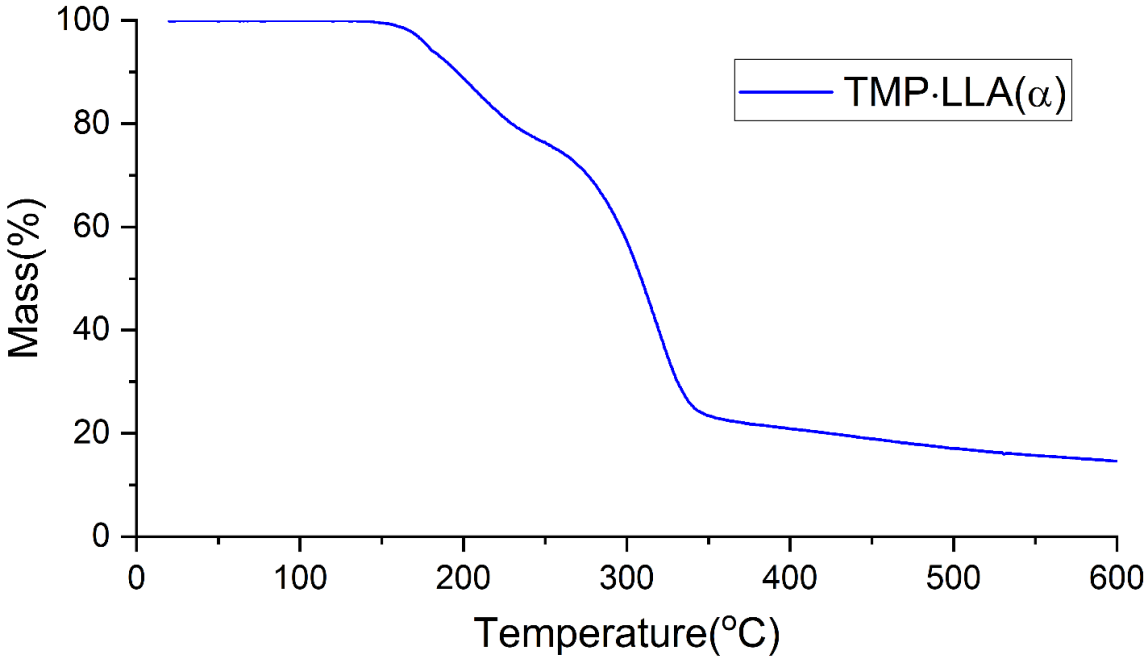

Fig. S12 TGA thermogram for **TMP·LLA(α)**. Crystal decomposition began at ca. 169 °C.

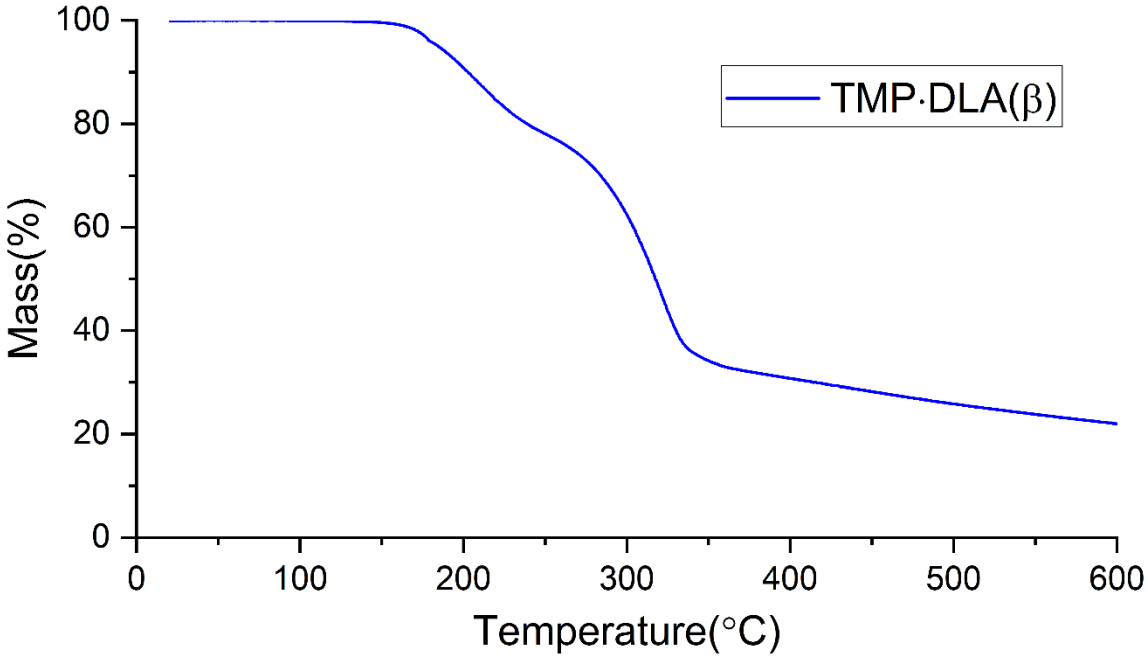

Fig. S13 TGA thermogram for **TMP·DLA(β)**. Crystal decomposition began at ca. 170 °C.

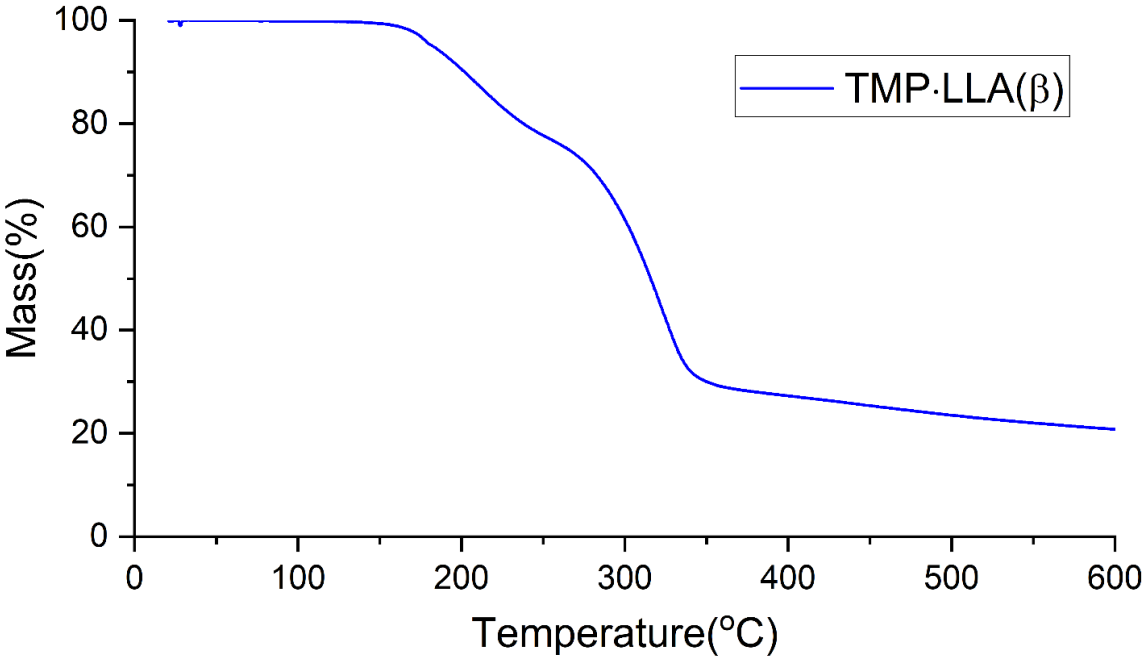

Fig. S14 TGA thermogram for **TMP·LLA(β)**. Crystal decomposition began at ca. 171 °C.

7. DTA data

DTA data was collected simultaneously with the TGA data by using a SHIMADZU DTG_60H instrument. An alumina cell and a nitrogen atmosphere were used. The flow rate was 100 mL/min, and the heating rate was 10 °C/min.

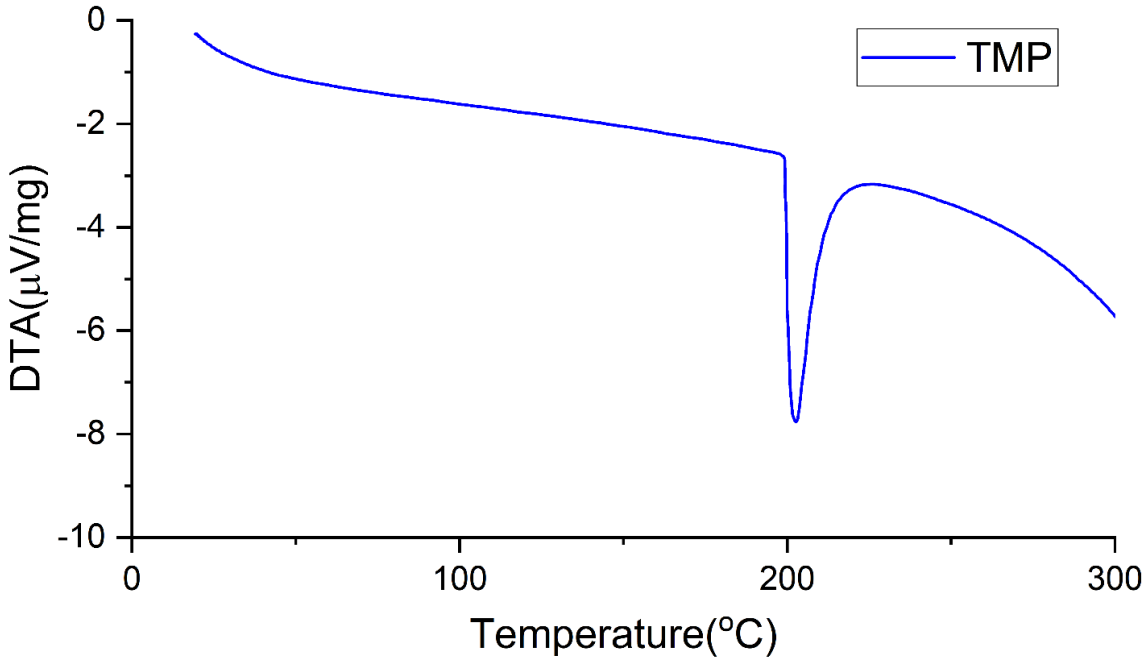

Fig. S15 DTA data for **TMP** (onset: 199 °C, peak: 203 °C).

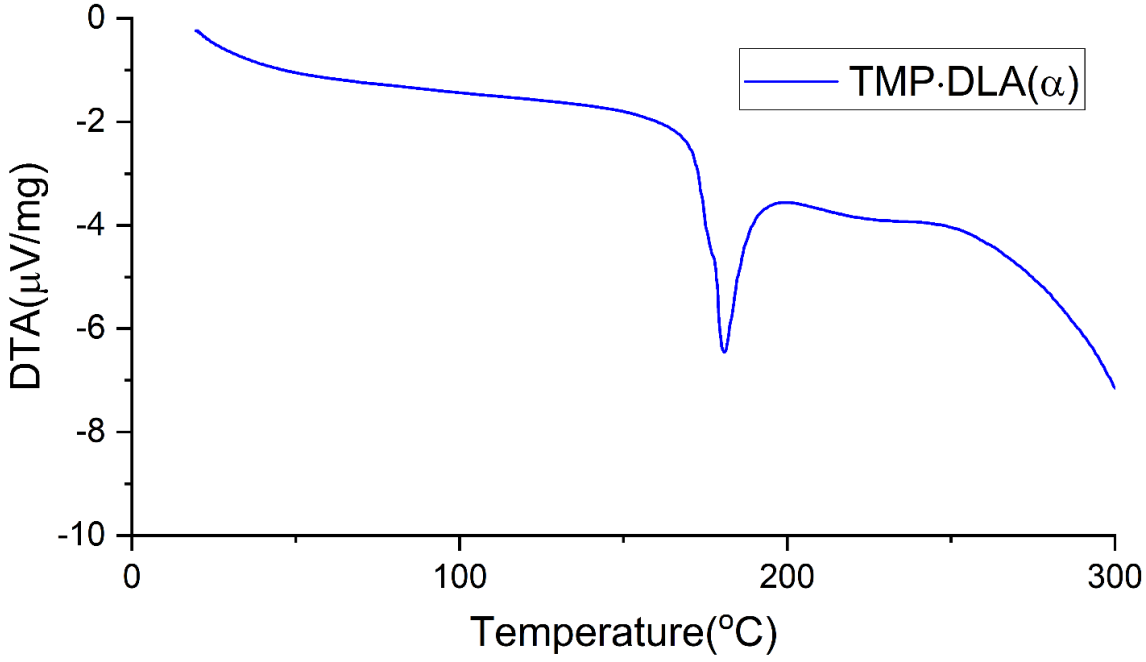

Fig. S16 DTA data for **TMP·DLA(α)** (onset: 176 °C, peak: 181 °C).

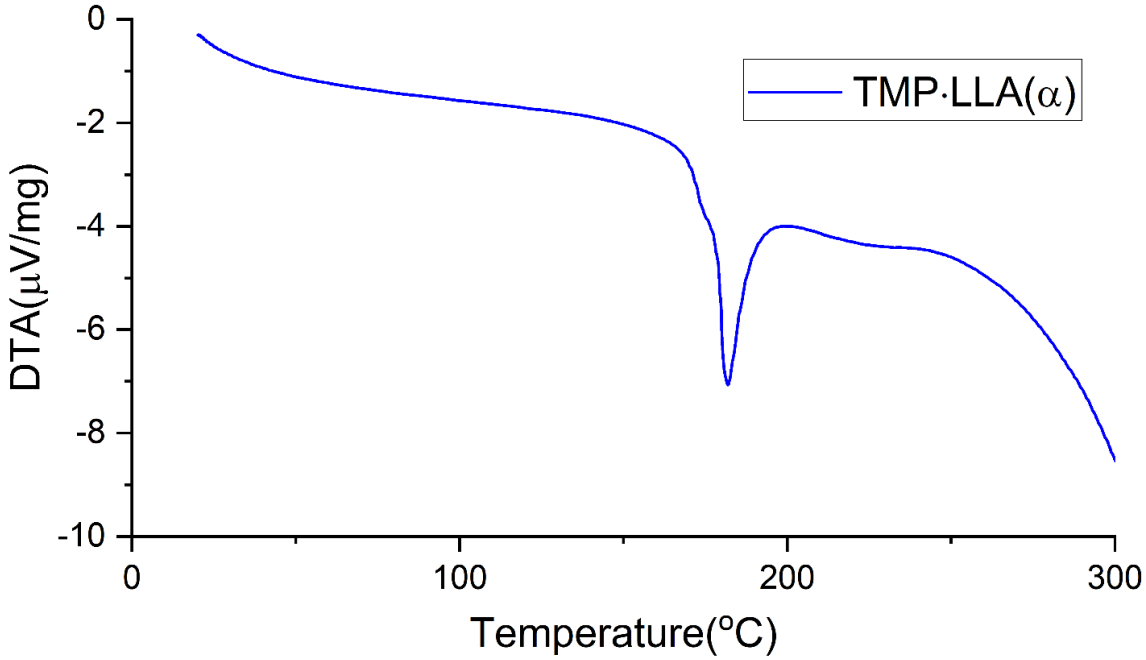

Fig. S17 DTA data for **TMP·LLA(α)** (onset: 178 °C, peak: 182 °C).

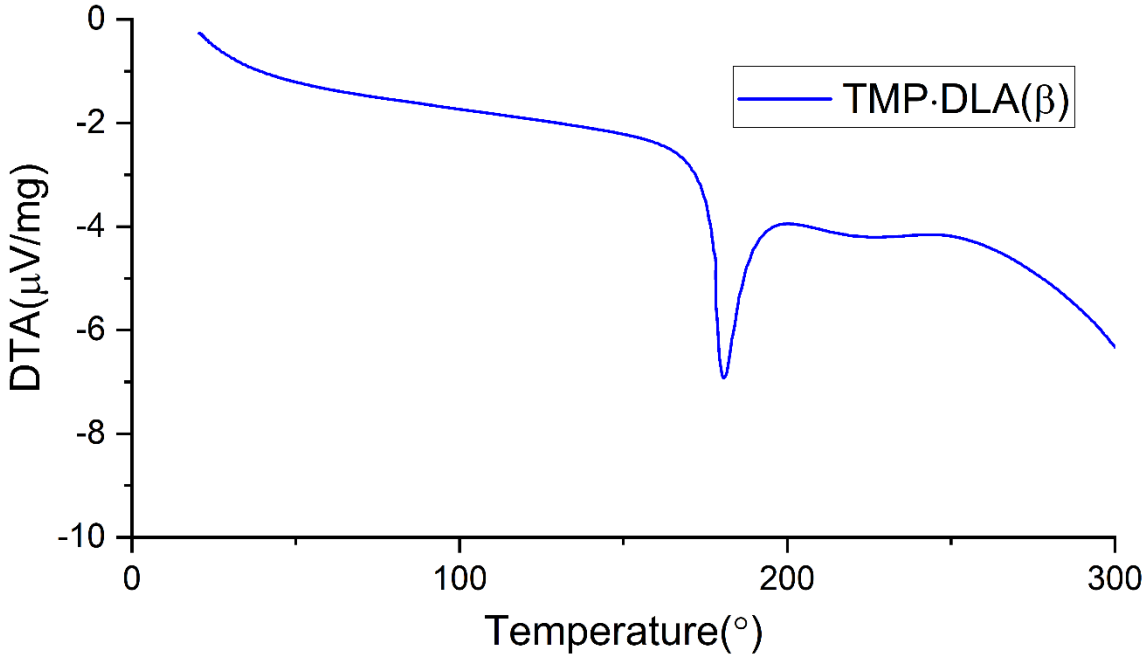

Fig. S18 DTA data for **TMP·DLA(β)** (onset: 177 °C, peak: 180 °C).

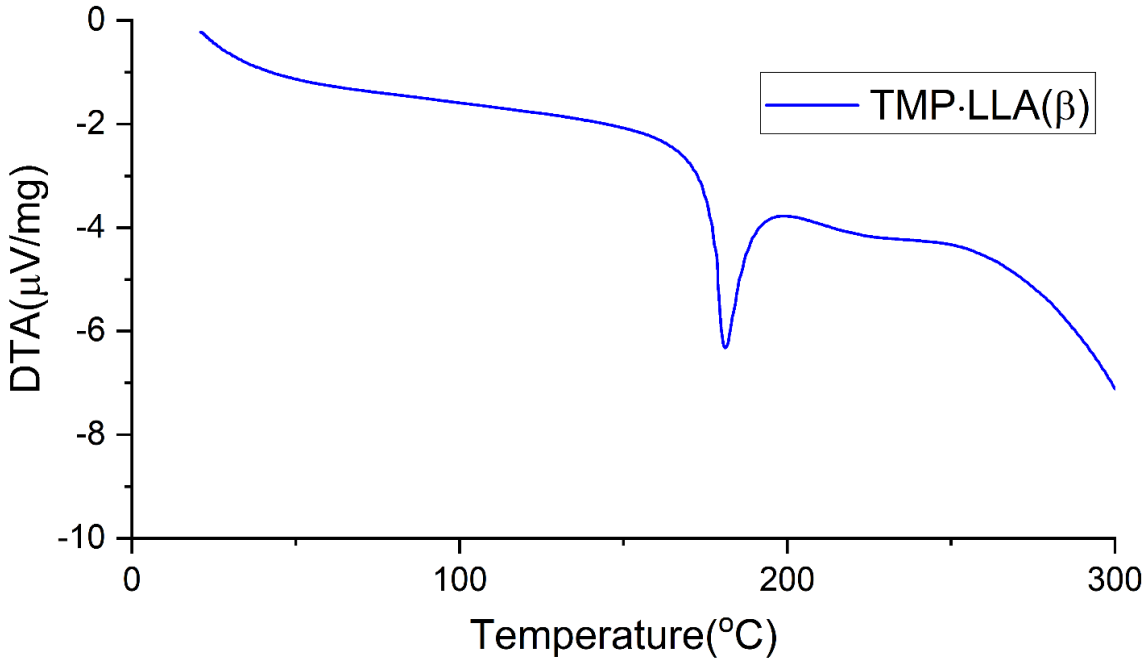

Fig. S19 DTA data for **TMP·LLA(β)** (onset: 177°C, peak: 181°C).

Table S3. Melting points (from DTA) and decomposition onset temperatures (from TGA) for **TMP** and the four salts.

Sample	Melting point (°C)	Decomposition onset temperature (°C)
TMP	199-203	278
TMP·DLA(α)	176-181	169
TMP·LLA(α)	178-182	169
TMP·DLA(β)	177-180	170
TMP·LLA(β)	177-181	171

8. FTIR spectra of components and salts

FTIR spectra were recorded on a Nicolet iS10 infrared spectrometer using an ATR attachment equipped with a diamond crystal.

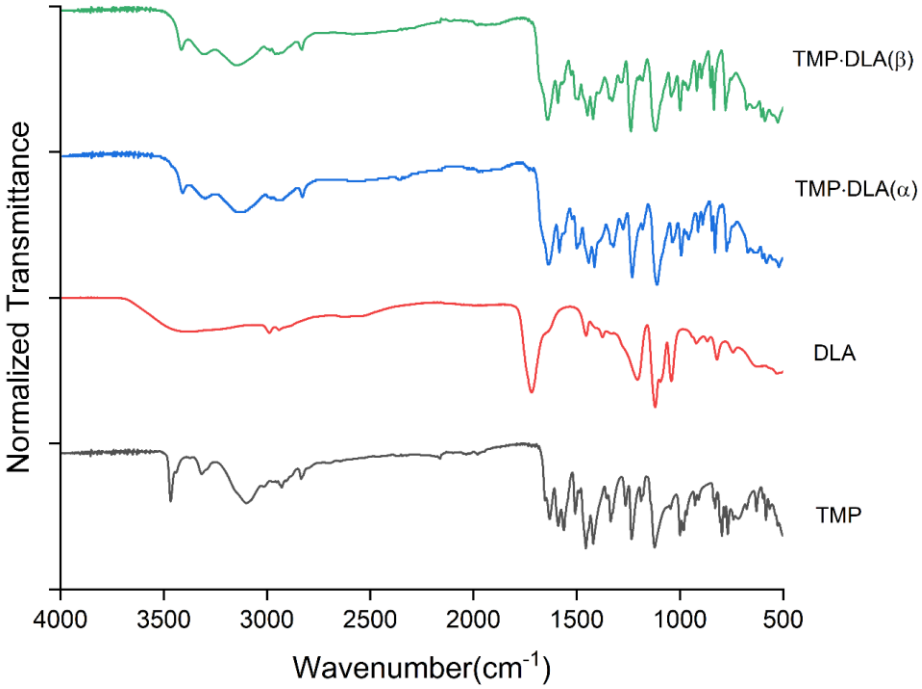

Fig. S20 FTIR spectra of **TMP**, **DLA**, **TMP·DLA(α)**, and **TMP·DLA(β)**.

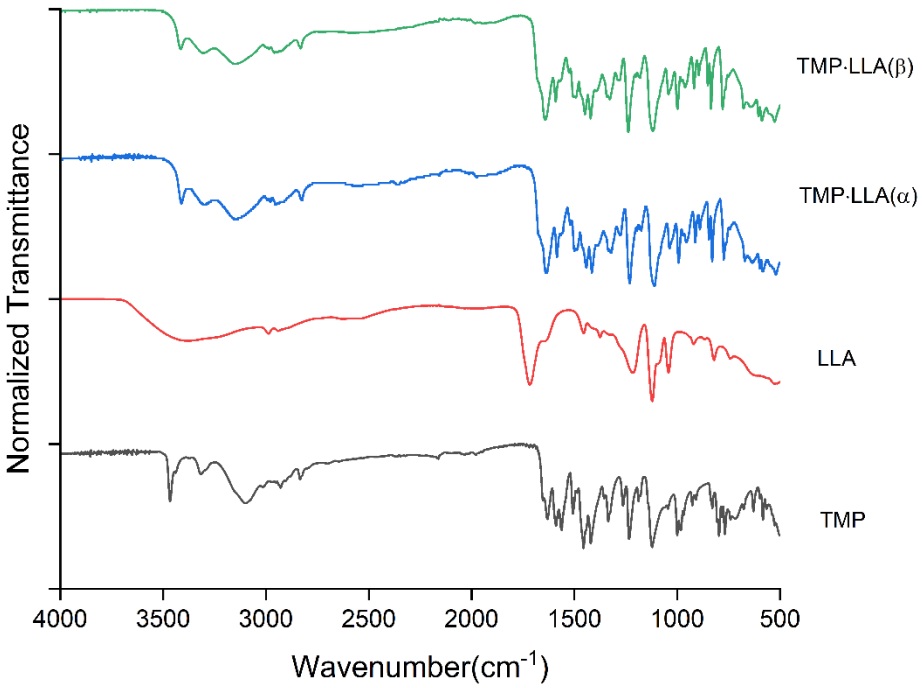

Fig. S21 FTIR spectra of **TMP**, **LLA**, **TMP·LLA(α)**, and **TMP·LLA(β)**.

9. Solubility studies

Solubility studies[6-8] were conducted using pH 1.2, 4.0, 7.4 buffers at 25 °C via shake-flask method. Excess amounts of the salts [**TMP·DLA(α)**, **TMP·LLA(α)**] and 2 mL buffer were added to 20 mL glass scintillation vials, then the vials were capped, and the mixtures were stirred and maintained at 25 ± 0.5 °C for 24 h. After that, the suspended solid was removed by filtration through Whatman membrane (0.45 µm pore size) syringe filter. The filtrate was appropriately diluted and analyzed by UV-Vis spectroscopy based on the Beer-Lambert law. The measurements were conducted on an Agilent 8453 UV-Vis Spectrophotometer using the maximum absorption wavelength of 271 nm (for pH 1.2 and pH 4.0) and 278 nm (for pH 7.4). The absorption coefficient of each salt was measured using the slope of absorbance vs concentration of the known concentrated solutions in pH 1.2, 4.0, and 7.4 buffers. The solubility of each polymorph of salts was determined as below.

Table S4. Solubility values (mg/mL) of **TMP** in different pH buffers.

Sample	TMP at pH 1.2	TMP at pH 4.0	TMP at pH 7.4
trial 1	3.39	21.53	0.54
trial 2	3.37	21.21	0.53
trial 3	3.38	21.34	0.55
average	3.38 ± 0.01	21.36 ± 0.16	0.54 ± 0.01

Table S5. Solubility values (mg/mL) of **TMP·DLA(α)** and **TMP·LLA(α)** in different pH buffers.

Sample	TMP·DLA(α) at pH 1.2	TMP·LLA(α) at pH 1.2	TMP·DLA(α) at pH 4.0	TMP·LLA(α) at pH 4.0	TMP·DLA(α) at pH 7.4	TMP·LLA(α) at pH 7.4
trial 1	3.57	3.45	97.50	95.62	1.10	0.99
trial 2	3.53	3.63	101.28	101.36	1.21	1.26
trial 3	3.88	3.70	103.40	100.88	1.29	1.32
average	3.66 ± 0.19	3.59 ± 0.13	100.73 ± 2.99	99.29 ± 3.18	1.20 ± 0.10	1.19 ± 0.18

10. PXRD patterns

The PXRD patterns for samples obtained through LAG and slurry experiments were collected on a Rigaku MiniFlex II powder diffractometer. The diffraction pattern was obtained by scanning a 2θ range of 3-50°, step size = 0.02°, and scan time of 2 degrees/minute. The X-ray source was Cu Kα radiation (λ =1.5418 Å) with an anode voltage of 30 kV and a current of 15 mA. Diffraction intensities were recorded on a position sensitive detector (D/teX Ultra). The sample was prepared as a standard powder mount, and the diffractogram was processed through the software MDI JADE 2020.

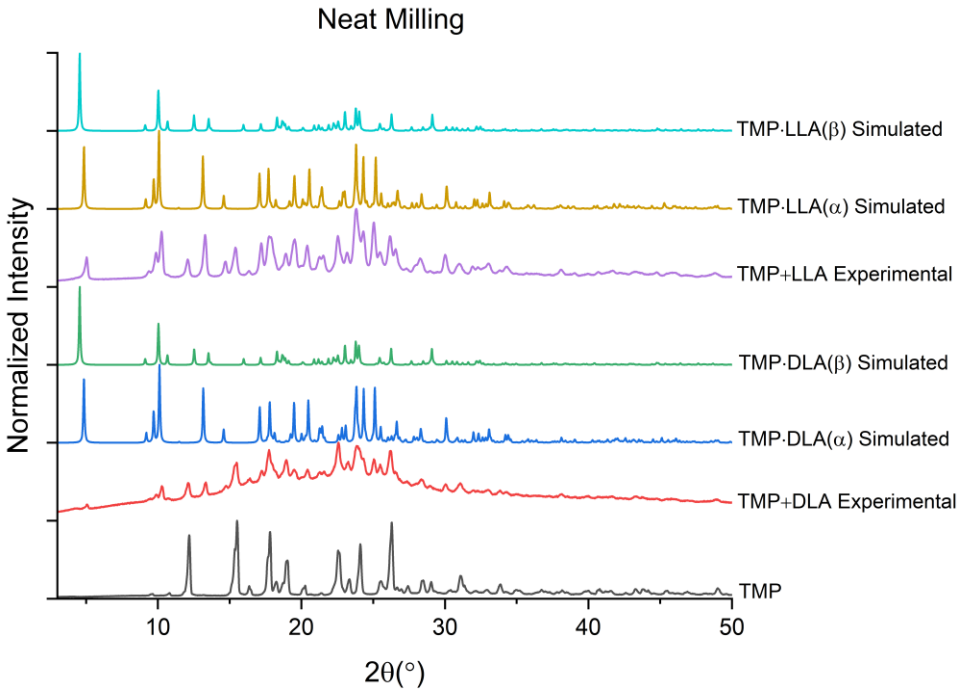

Fig. S22 PXRD patterns of solids obtained through neat milling experiments for **TMP+DLA** and **TMP+LLA**. Simulated patterns of **TMP·DLA(α)**, **TMP·DLA(β)**, **TMP·LLA(α)**, **TMP·LLA(β)** from single-crystal X-ray data for each salt at 100 K, and **TMP** are shown.

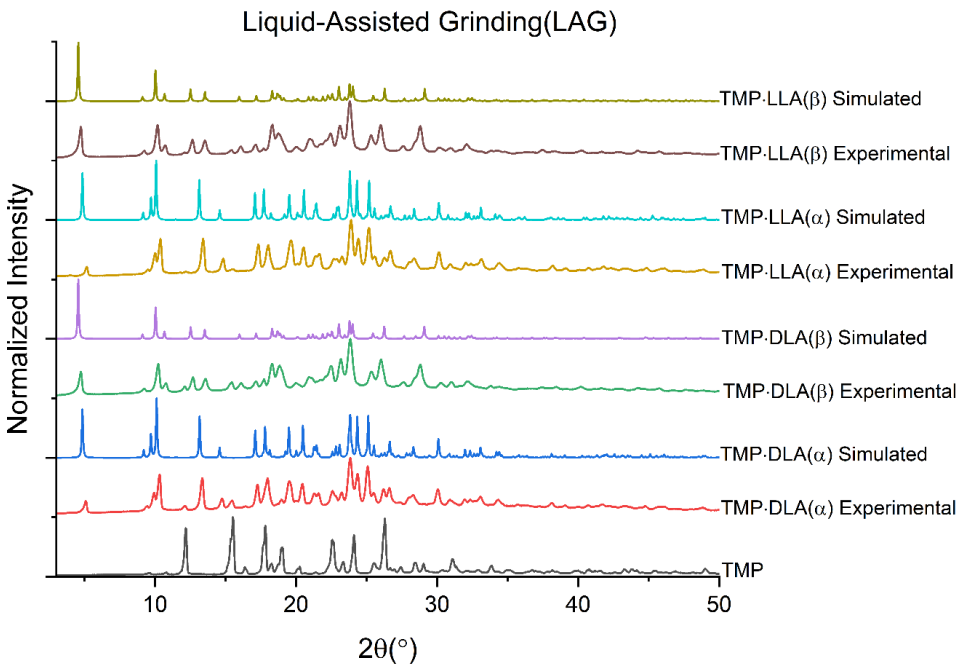

Fig. S23 PXRD patterns of solids obtained through LAG experiments via two different solvents (ethanol for alpha and acetonitrile for beta) for **TMP·DLA(α)**, **TMP·DLA(β)**, **TMP·LLA(α)**, **TMP·LLA(β)**, simulated patterns from single-crystal X-ray data for each salt at 100 K, and **TMP**.

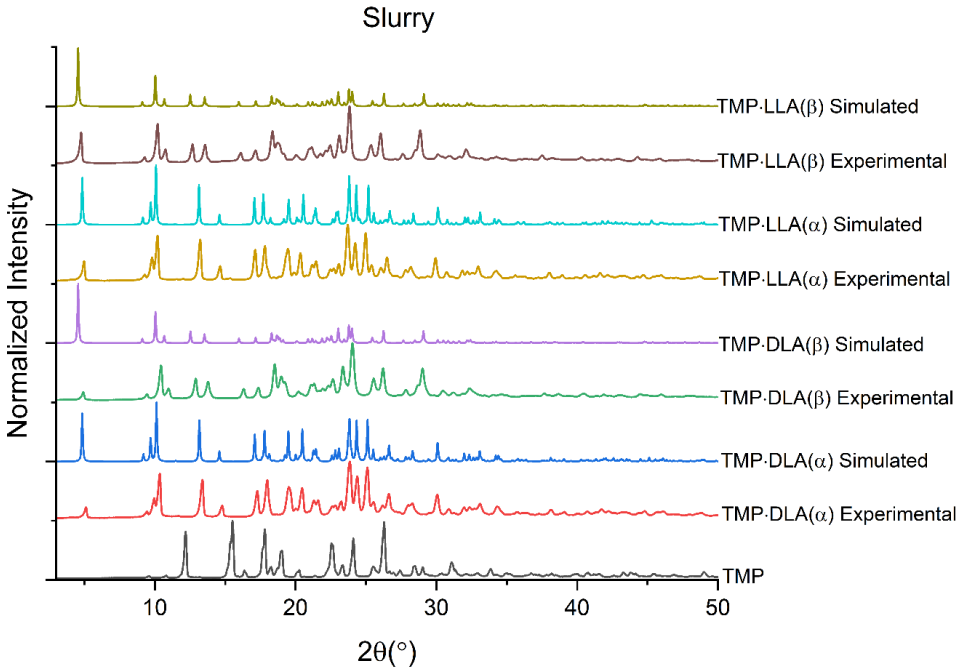

Fig. S24 PXRD patterns of solids obtained through slurry experiments via two different solvents (ethanol for alpha and acetonitrile for beta) for **TMP·DLA(α)**, **TMP·DLA(β)**, **TMP·LLA(α)**, **TMP·LLA(β)**, simulated patterns from single-crystal X-ray data for each salt at 100 K, and **TMP**.

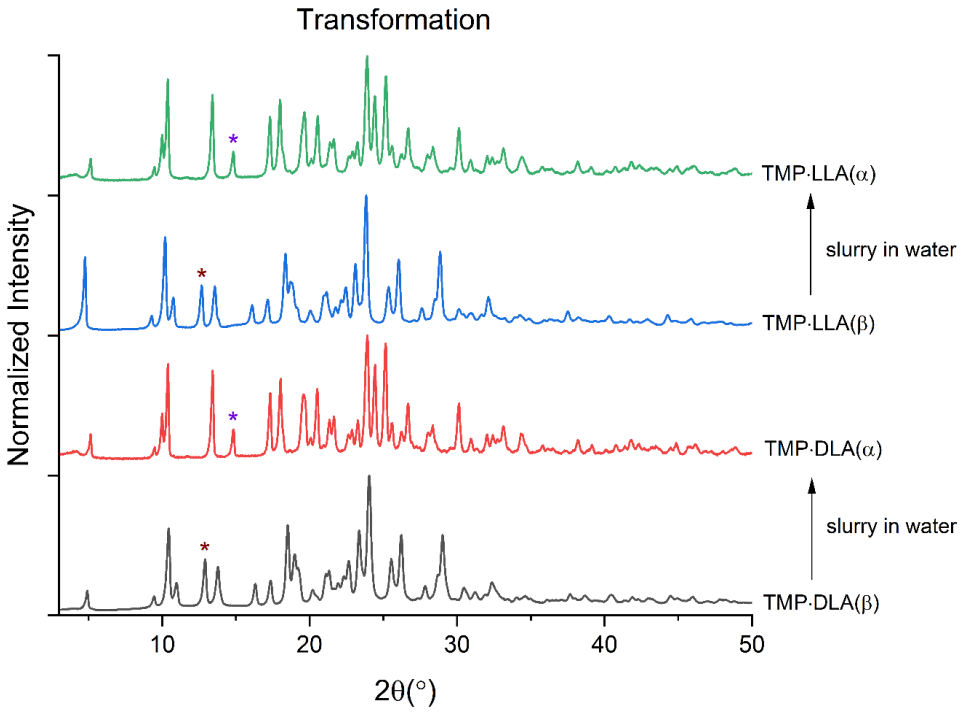

Fig. S25 PXRD patterns showing transformation of **TMP·DLA** and **TMP·LLA** salts from beta to alpha polymorphs in water. The specific peaks used to distinguish alpha from beta are starred.

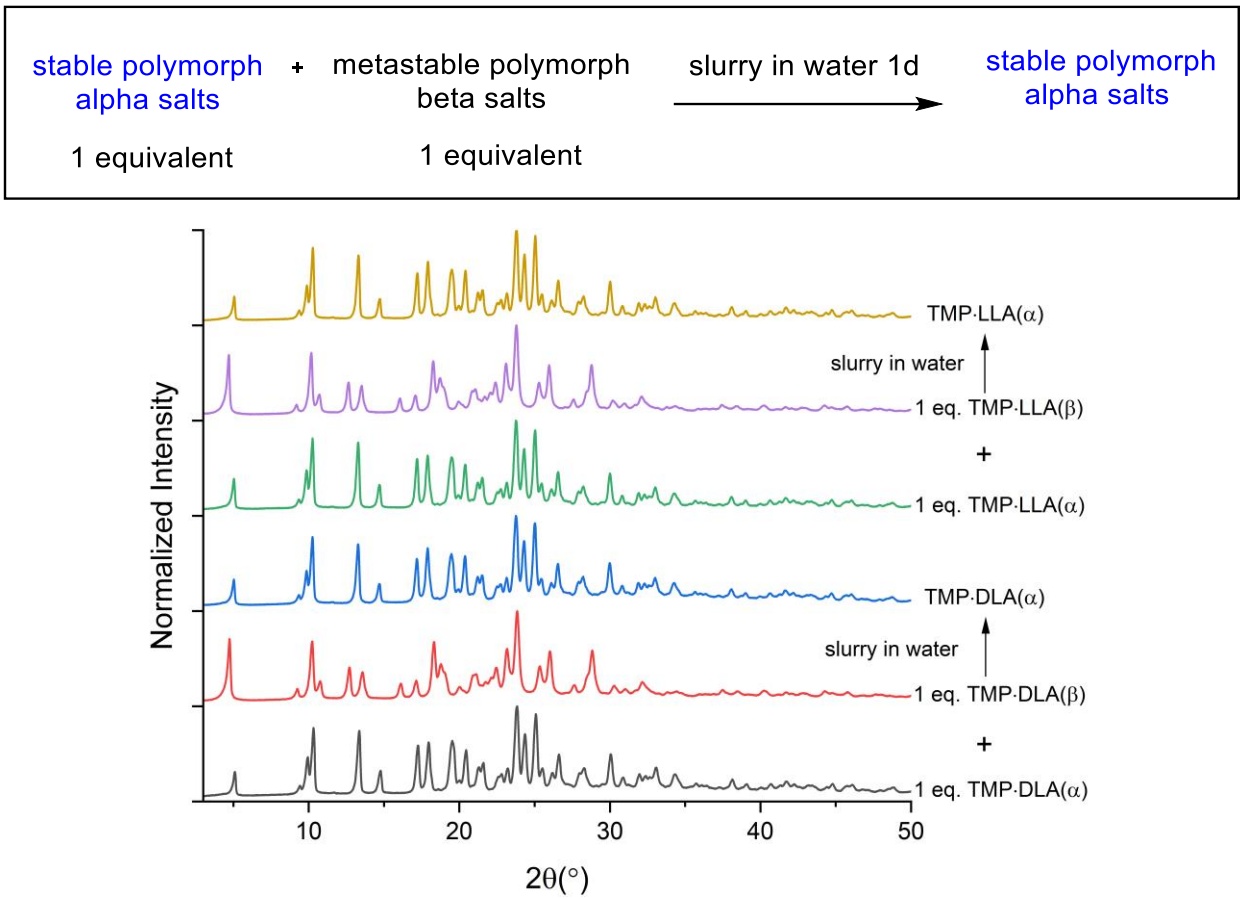

Fig. S26 PXRD patterns of **TMP·DLA(α)**, **TMP·DLA(β)**, and slurry experiments of 1:1 **TMP·DLA(α)**:**TMP·DLA(β)** salts after 1d stirring in water; **TMP·LLA(α)**, **TMP·LLA(β)**, and 1:1 **TMP·LLA(α)**:**TMP·LLA(β)** salts after 1d stirring in water.

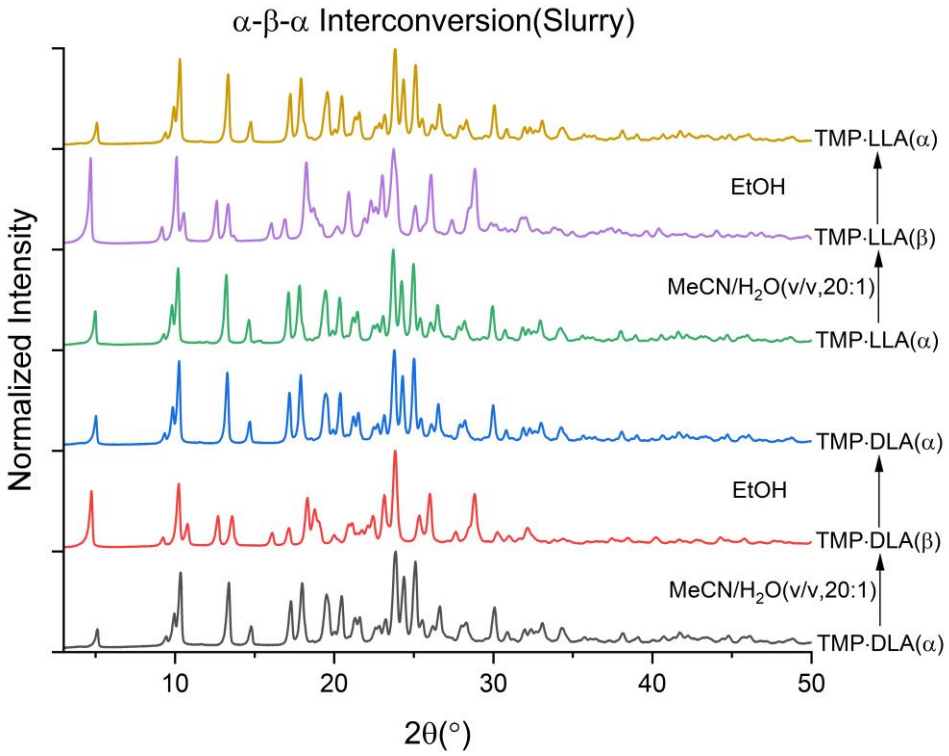

Fig. S27 PXRD patterns obtained through slurry experiments showing a full cycle of interconversion of **TMP·DLA** and **TMP·LLA** salts (alpha to beta to alpha).

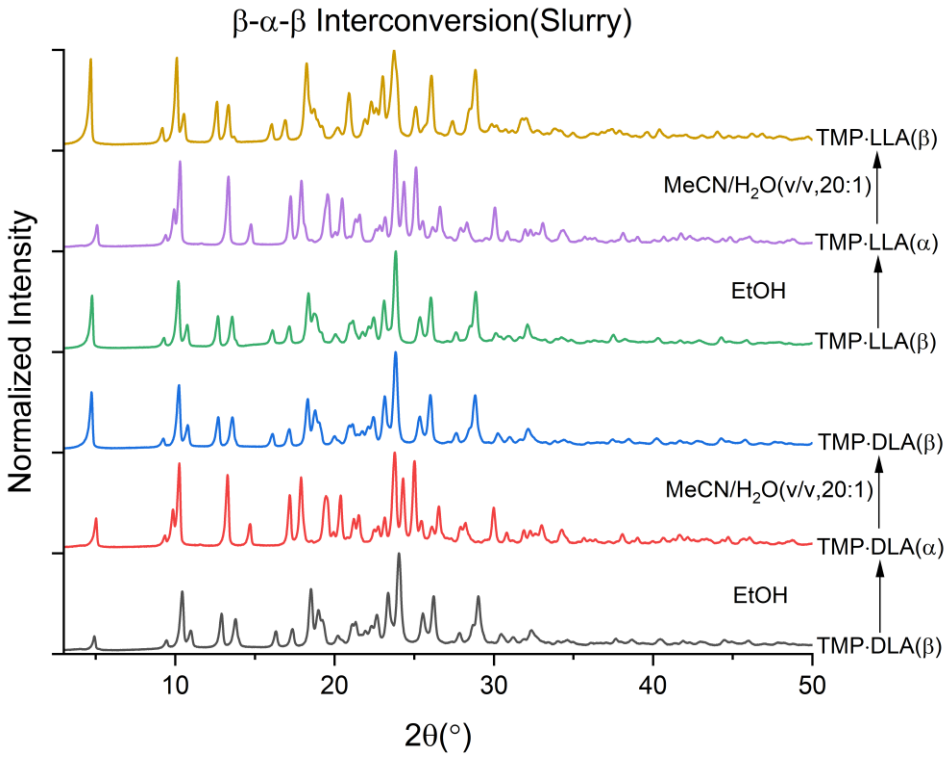

Fig. S28 PXRD patterns obtained through slurry experiments showing a full cycle of interconversion of **TMP·DLA** and **TMP·LLA** salts (beta to alpha to beta).

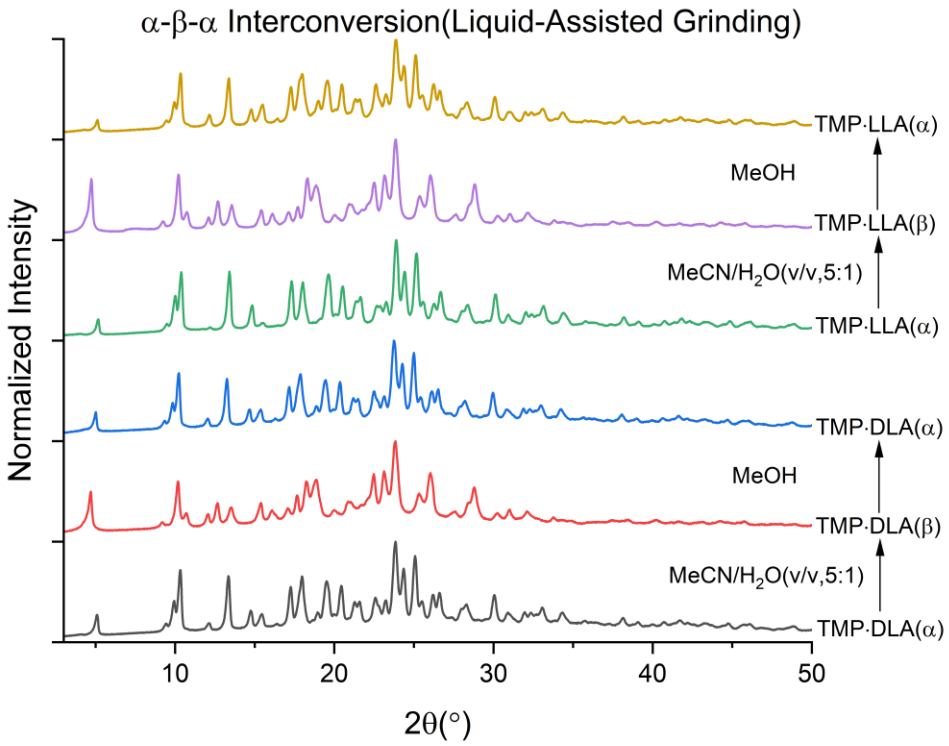

Fig. S29 PXRD patterns obtained through LAG experiments showing a full cycle of interconversion of **TMP·DLA** and **TMP·LLA** salts (alpha to beta to alpha).

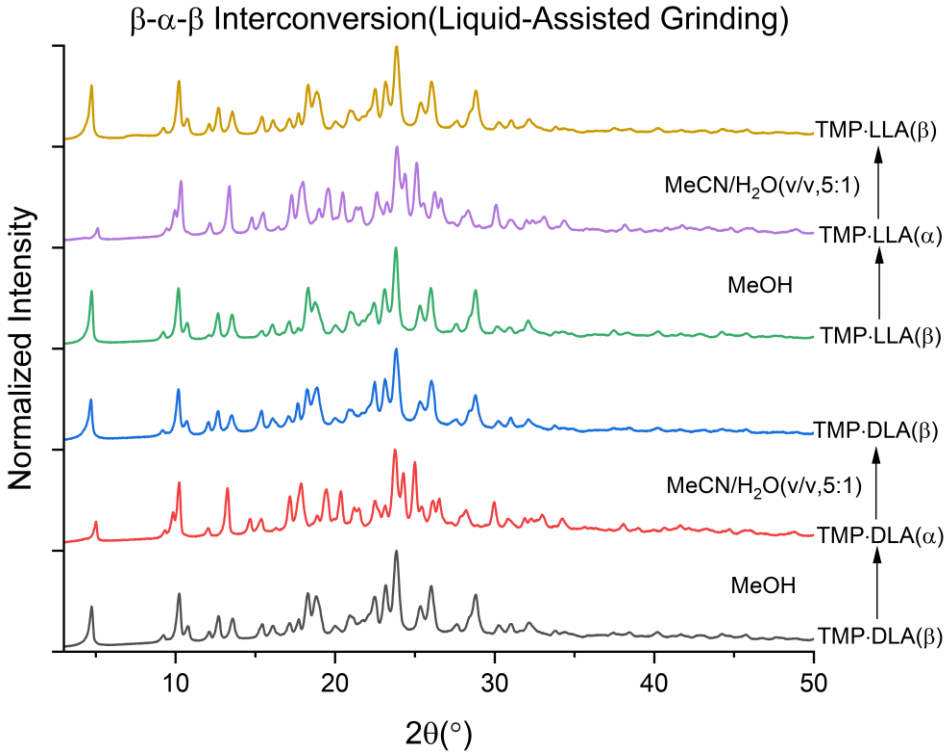

Fig. S30 PXRD patterns obtained through LAG experiments showing a full cycle of interconversion of **TMP·DLA** and **TMP·LLA** salts (beta to alpha to beta).

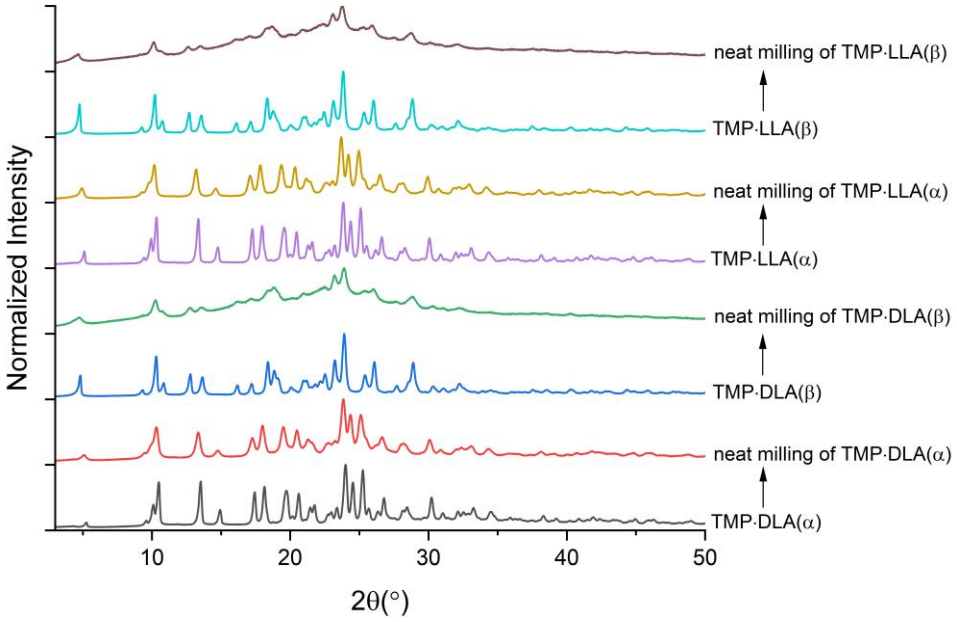

Fig. S31 PXRD patterns of **TMP·DLA(α)**, **TMP·DLA(β)**, **TMP·LLA(α)**, **TMP·LLA(β)**, and each powder after 15 min neat milling.

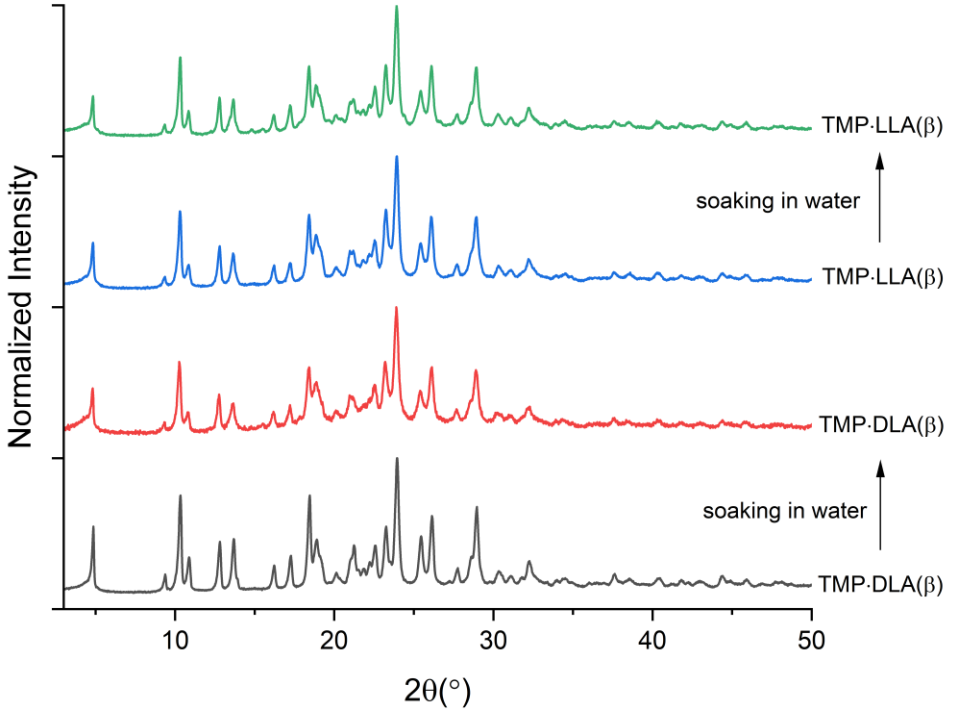

Fig. S32 PXRD patterns of **TMP·DLA(β)**, **TMP·LLA(β)** and soaking experiments of **TMP·DLA(β), TMP·LLA(β)** after soaking in water overnight without stirring.

11. Crystal imaging experiments

Excess crystalline powders of the beta forms of **TMP** salts and 0.5 mL H_2O were added in a DRAM vial with a stir bar. After a one-hour slurry, the mother liquid was obtained by filtration through Fisherbrand membrane (0.2 μm pore size) syringe filter. One drop of mother liquid and several **TMP·DLA(β)** crystals were added to a glass slide with a round glass side covering it. After 5, 10, and 30 minutes, optical images were collected on a Leica DM2700 M microscope equipped with a Leica MC170 HD microscope camera.

An example set of images from one experiment is shown below. Unit cell analysis performed on single crystals after exposure to liquid without application of mechanical force showed no polymorph conversion.

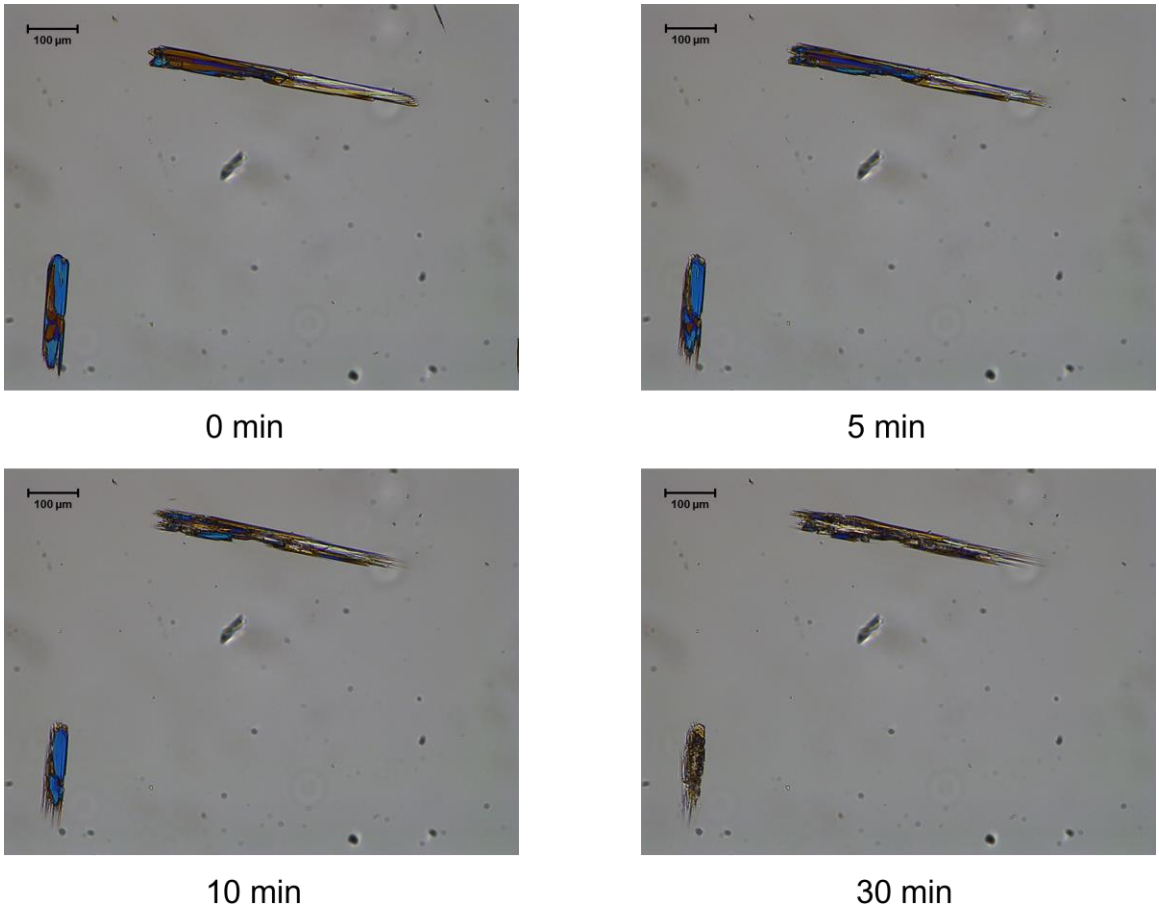

Fig. S33 Optical microscope images of **TMP·DLA(β)** crystals soaking in one drop of mother liquid after 5, 10, and 30 minutes.

12. References

1. CrysAlis^{Pro} (2018) Oxford Diffraction Ltd.

2. SCALE3 ABSPACK (2005) Oxford Diffraction Ltd.

3. G. M. Sheldrick, *Acta Crystallogr., Sect. A: Found. Adv.* 2015, **A71**, 3-8.

4. G.M. Sheldrick, *Acta Crystallogr., Sect. C: Struct. Chem.* 2015, ***C71***, 3-8.

5. O. V. Dolomanov, L. J. Bourhis, R. J. Gildea, J. A. Howard and H. Puschmann, *J. Appl. Cryst*. 2009, **42**, 339-341.

6. E. Baka, J. E. Comer and K. Takács-Novák, *J. Pharm. Biomed. Anal*. 2008, **46**, 335-341.

7. S. P. Gopi, S. Ganguly and G. R. Desiraju, *Mol. Pharm.* 2016, **13**, 3590-3594.

8. R. M. Obaidat, M. Khanfar and R. Ghanma, *AAPS PharmSciTech.* 2019, **20**, 1-13.